

Time-of-flight method using multiple pulse train interference as a time recorder

Dong Wei,^{1,*} Satoru Takahashi,¹ Kiyoshi Takamasu,¹ and Hirokazu Matsumoto¹

¹*Department of Precision Engineering, University of Tokyo, Hongo 7-3-1, Bunkyo-ku, Tokyo 113-8656, Japan*

**weidong@nanolab.t.u-tokyo.ac.jp*

Abstract: A unique length measurement method, called the multiple pulse train interference-based time-of-flight (TOF) method, is proposed and demonstrated for the first time. By taking advantage of both the high-accuracy measurement capability of a pulse train interference method and the arbitrary and absolute length measurement capability of a TOF method, the present method is expected to be useful for high-precision length measurement for not only science purposes but also industry requirements. A long gauge block was measured using this optical method to demonstrate the feasibility of the proposed method.

©2011 Optical Society of America

OCIS codes: (120.0120) Instrumentation, measurement, and metrology; (140.4050) Mode-locked lasers; (030.1640) Coherence; (120.2830) Interferometry; (120.3940) Metrology.

References and links

1. T. Araki, "Optical distance meter using a short pulse width laser diode and a fast avalanche photodiode," *Rev. Sci. Instrum.* **66**(1), 43–47 (1995), http://rsi.aip.org/resource/1/rsinak/v66/i1/p43_s1.
2. A. Kilpelä, R. Pennala, and J. Kostamovaara, "Precise pulsed time-of-flight laser range finder for industrial distance measurements," *Rev. Sci. Instrum.* **72**(4), 2197–2202 (2001), http://rsi.aip.org/resource/1/rsinak/v72/i4/p2197_s1.
3. R. Illingworth, and I. S. Ruddock, "Cavity length measurement for synchronously pumped, mode-locked lasers," *Opt. Commun.* **59**(5-6), 375–378 (1986).
4. A. M. Chekhovsky, A. N. Golubev, and M. V. Gorbunkov, "Optical pulse distance-multiplying interferometry," *Appl. Opt.* **37**(16), 3480–3483 (1998), <http://www.opticsinfobase.org/ao/abstract.cfm?uri=ao-37-16-3480>.
5. L. Rovati, U. Minoni, M. Bonardi, and F. Docchio, "Absolute distance measurement using comb-spectrum interferometry," *J. Opt.* **29**(3), 121–127 (1998), <http://iopscience.iop.org/0150-536X/29/3/004>.
6. J. Ye, "Absolute measurement of a long, arbitrary distance to less than an optical fringe," *Opt. Lett.* **29**(10), 1153–1155 (2004), <http://www.opticsinfobase.org/abstract.cfm?URI=ol-29-10-1153>.
7. K. N. Joo, and S. W. Kim, "Absolute distance measurement by dispersive interferometry using a femtosecond pulse laser," *Opt. Express* **14**(13), 5954–5960 (2006), <http://www.opticsinfobase.org/abstract.cfm?URI=oe-14-13-5954>.
8. M. Cui, R. N. Schouten, N. Bhattacharya, and S. A. Berg, "Experimental demonstration of distance measurement with a femtosecond frequency comb laser," *J. Europ. Opt. Soc. Rap. Public.* **3**, 08003 (2008), https://www.jeos.org/index.php/jeos_rp/article/view/08003/246.
9. P. Balling, P. Kren, P. Masika, and S. A. van den Berg, "Femtosecond frequency comb based distance measurement in air," *Opt. Express* **17**(11), 9300–9313 (2009), <http://www.opticsinfobase.org/abstract.cfm?uri=oe-17-11-9300>.
10. M. Cui, M. G. Zeitouny, N. Bhattacharya, S. A. van den Berg, H. P. Urbach, and J. J. M. Braat, "High-accuracy long-distance measurements in air with a frequency comb laser," *Opt. Lett.* **34**(13), 1982–1984 (2009), <http://www.opticsinfobase.org/abstract.cfm?uri=ol-34-13-1982>.
11. J. Lee, Y.-J. Kim, K. Lee, S. Lee, and S.-W. Kim, "Time-of-flight measurement with femtosecond light pulses," *Nat. Photonics* **4**(10), 716–720 (2010), <http://www.nature.com/nphoton/journal/v4/n10/full/nphoton.2010.175.html>.
12. D. Wei, S. Takahashi, K. Takamasu, and H. Matsumoto, "Analysis of the temporal coherence function of a femtosecond optical frequency comb," *Opt. Express* **17**(9), 7011–7018 (2009), <http://www.opticsinfobase.org/abstract.cfm?uri=oe-17-9-7011>.
13. D. Wei, S. Takahashi, K. Takamasu, and H. Matsumoto, "Simultaneous observation of high temporal coherence between two pairs of pulse trains using a femtosecond-optical-frequency-comb-based interferometer," *Jpn. J. Appl. Phys.* **48**(7), 070211 (2009), <http://jjap.jsap.jp/link?JJAP/48/070211/>.
14. D. Wei, S. Takahashi, K. Takamasu, and H. Matsumoto, "Experimental observation of pulse trains' destructive interference with a femtosecond optical frequency-comb-based interferometer," *Opt. Lett.* **34**(18), 2775–2777 (2009), <http://ol.osa.org/abstract.cfm?URI=ol-34-18-2775>.

15. D. Wei, S. Takahashi, K. Takamasu, and H. Matsumoto, "Femtosecond optical frequency comb-based tandem interferometer," *J. Europ. Opt. Soc. Rap. Public.* **4**, 09043 (2009), https://www.jeos.org/index.php/jeos_rp/article/view/09043.
 16. F. Helbing, G. Steinmeyer, and U. Keller, "Carrier-envelope offset phase-locking with attosecond timing jitter," *IEEE J. Quantum Electron.* **9**(4), 1030–1040 (2003), http://ieeexplore.ieee.org/xpls/abs_all.jsp?arnumber=1250460&tag=1.
 17. D. Wei, S. Takahashi, K. Takamasu, and H. Matsumoto, "Theoretical analysis of length measurement using interference of multiple pulse trains of a femtosecond optical frequency comb," *Jpn. J. Appl. Phys.* (to be published).
 18. Y. Yamaoka, K. Minoshima, and H. Matsumoto, "Direct measurement of the group refractive index of air with interferometry between adjacent femtosecond pulses," *Appl. Opt.* **41**(21), 4318–4324 (2002), <http://ao.osa.org/abstract.cfm?URI=ao-41-21-4318>.
-

1. Introduction

In July 2009, the national standard tool for measuring length in Japan changed from an iodine-stabilized helium-neon (He-Ne) laser to a femtosecond optical frequency comb (FOFC). Because length measurements based on length standards are mandatory to meet not only science purposes but also industry requirements, the determination of how to practically perform a distant metrology that is directly linked to an FOFC length standard tool is an urgent challenge.

The time-of-flight (TOF) method is a well-known procedure that uses a pulse laser for an arbitrary and absolute length measurement (for example, see [1,2]). The principle of the TOF method is based on the fact that the length is a product of the multiplication of the time difference and the light velocity. The time difference is obtained by measuring two time points, the time point when the pulse exits the measuring instrument, and the time point when the pulses come back to the measuring instrument after being reflected by the object. Because an FOFC is a pulse laser, the FOFC-based TOF method is promising; however, the measurement accuracy of the two time points is decided by the conversion accuracy from the light signal into an electric signal, and thus it is difficult to achieve better than millimeter-scale accuracy.

Recently, several attempts to measure distance by observing the cross-correlation functions between different pulse trains have been made [3–11]. In all of these previous works, the observed interference was restricted to only one pair of pulse trains.

In our previous work, in discussing the phenomenon "why different pulse trains can interfere with each other", we have investigated the temporal coherence function of a pulse train from an FOFC [12]. Our results [13–15] showed that high temporal coherence peaks exist during the period equal to the repetition intervals in the traveling direction of the FOFC.

The proposed method in the current study works as follows. The TOF method can measure an arbitrary and absolute length, but the accuracy is worse than that of the pulse train interference method [3–11]. The pulse train interference method, however, can only measure a discrete distance. By taking advantage of both the TOF method and the pulse train interference method, we record both time points of the TOF method by using different pulse train interference instances and analyze the multiple pulse train interference fringes for length information, to measure an arbitrary and absolute length with high accuracy.

Based on this consideration, in the present study, we demonstrate a multiple pulse train interference-based (MPTI-based) TOF method. For simplicity of explanation, we have neglected the dispersion and absorption of the optical devices that occur in the FOFC's illumination bandwidth.

2. Principles

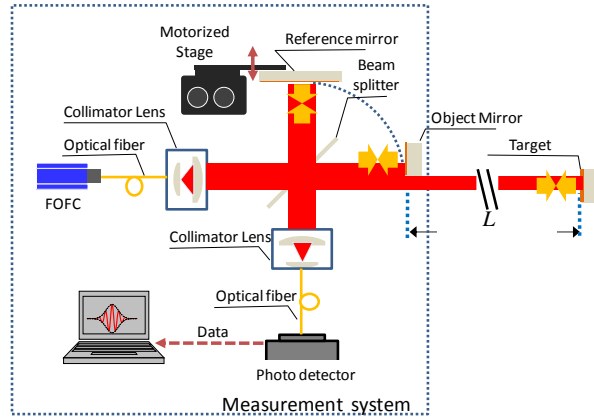


Fig. 1. System overview of the MPTI-based TOF method. FOFC: femtosecond optical frequency comb.

Figure 1 shows the system overview of the MPTI-based TOF method. The optical scheme is carried out with a system consisting of an FOFC optical source, a modified Michelson interferometer, and system controls.

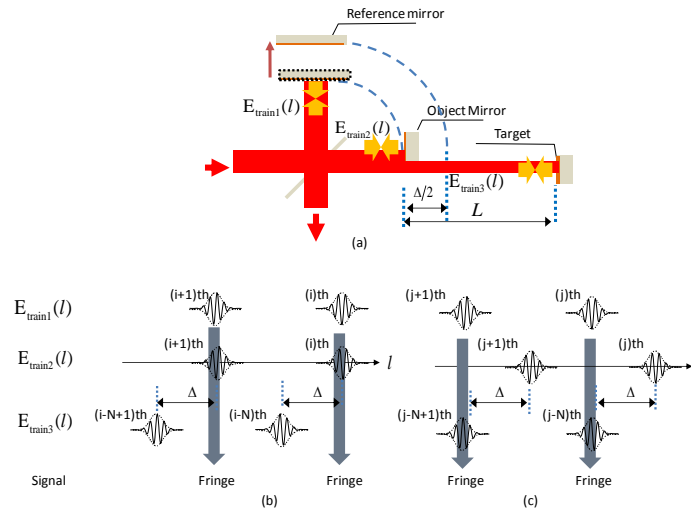


Fig. 2. Interference fringes form with different relative delays between pulse trains formed by the interferometer. With a relative optical-path delay of 0 and Δ , the relatively delayed pulse trains will overlap as shown in (b) and (c), respectively, and the expected interference fringes can be observed.

The features of an FOFC can be summarized as follows [16]: In the frequency domain, a mode-locked laser generates equidistant frequency comb lines with the pulse repetition frequency f_{rep} , and the whole equidistant frequency comb is shifted by offset frequency f_{CEO} from zero frequency. In the time domain, when the electric field packet repeats at the pulse repetition period $T_R = 1/f_{\text{rep}}$, due to offset frequency f_{CEO} , the carrier phase slips by $\Delta\varphi_{\text{ce}} = 2\pi f_{\text{CEO}} / f_{\text{rep}}$ to the carrier-envelope phase.

As shown in Fig. 1, the pulse train from an FOFC light source is introduced into the modified Michelson interferometer to observe the MPTI fringes, and this system is used as a time recorder of the TOF method. The modified Michelson interferometer is a combination of

an ordinary Michelson interferometer and an unbalanced optical-path Michelson interferometer. The ordinary Michelson interferometer is composed of a beam splitter, a reference mirror, and an object mirror. The ordinary Michelson interferometer is used to record the time point when the pulse exits the measurement system. The unbalanced Michelson interferometer is composed of the same beam splitter and reference mirror, and a different object mirror as a target. The target is located far from the front surface of the reference mirror at an arbitrary and absolute distance L in space. The unbalanced Michelson interferometer is used to record the time point when the pulse is reflected by the target and comes back to the measurement system.

An arbitrary and absolute distance L between the object mirror and the target can be expressed as follows:

$$L = (N \times c_n \times T_R + \Delta) / 2. \quad (1)$$

Where N and Δ denote an integer ($N = 0, 1, 2, 3, \dots$) and an excess fraction ($c_n \times T_R < \Delta \leq 0$), respectively. Here, $N = \text{floor}[2L/(c_n \times T_R)]$ ($\text{floor}[2L/(c_n \times T_R)]$ rounds the elements of $2L/(c_n \times T_R)$ to the nearest integers less than or equal to $2L/(c_n \times T_R)$), $\Delta = \text{mod}(2L, N \times c_n \times T_R)$ returns $2L - N \times c_n \times T_R$, and c_n is the light velocity in air.

Next, we consider how to determine N and Δ form the MPTI fringes for a measurement of the arbitrary and absolute distance L . As shown in Fig. 2(a), the pulse train is split into two identical parts at the beam splitter. One part of the pulse train, $E_{\text{train1}}(l)$, goes into the common reference arm of the two interferometers and is reflected by the reference mirror. The other part of the pulse train goes into the other arm with lengths l and $l+L$ and is sequentially reflected by the object mirror ($E_{\text{train2}}(l)$) and the target ($E_{\text{train3}}(l)$), respectively. These two pairs of pulse trains, ($E_{\text{train1}}(l)$ and $E_{\text{train2}}(l)$) (Fig. 2(b)), ($E_{\text{train1}}(l)$ and $E_{\text{train3}}(l)$) (Fig. 2(c)), are finally recombined at the beam splitter.

During the measurement, by moving the common reference mirror of the two interferometers, we can observe the following MPTI fringes [17]:

$$\begin{aligned} I(l) &= a_1 + b_1 \times \exp\left[-\left(2\sqrt{\ln 2}l/L_{\text{coh}}\right)^2\right] \times \cos(k \times l) \\ &+ a_2 + b_2 \times \exp\left[-\left(2\sqrt{\ln 2}(l+\Delta)/L_{\text{coh}}\right)^2\right] \times \cos(k \times (l+\Delta) - N \times \Delta\phi_{\text{ce}}) \\ &= I_1(l) + I_2(l) \end{aligned} \quad (2)$$

Here

$$\begin{aligned} I_1(l) &= a_1 + b_1 \times \exp\left[-\left(2\sqrt{\ln 2}l/L_{\text{coh}}\right)^2\right] \times \cos(k \times l), \\ I_2(l) &= a_2 + b_2 \times \exp\left[-\left(2\sqrt{\ln 2}(l+\Delta)/L_{\text{coh}}\right)^2\right] \times \cos(k \times (l+\Delta) - N \times \Delta\phi_{\text{ce}}). \end{aligned} \quad (3)$$

In Eq. (2), $a_{1,2} = I_{\text{ref}} + I_{\text{obj1,2}}$ and $b_{1,2} = 2\sqrt{I_{\text{ref}} I_{\text{obj1,2}}}$, and I_{ref} , I_{obj1} , and I_{obj2} are the intensities reflected by the reference mirror, object mirror, and target, respectively. In addition, we assume that the FOFC source used shows a Gaussian spectral distribution, and L_{coh} is the temporal coherence length of one pulse.

In Eq. (3), $I_1(l)$ is the conventional white light (same pulse train) interference fringes formed by $E_{\text{train1}}(l)$ and $E_{\text{train2}}(l)$, and $I_2(l)$ is the different pulse trains interference fringes formed by $E_{\text{train1}}(l)$ and $E_{\text{train3}}(l)$.

Note that in the frequency domain, the offset shift frequency, f_{ceo} , and the pulse repetition frequency, f_{rep} , are the only two key parameters used to stabilize an FOFC. To perform

extreme-precision frequency metrology, the offset shift frequency, f_{CEO} , and the pulse repetition frequency, f_{rep} , must be stabilized, which means the pulse repetition period, $T_R = 1/f_{\text{rep}}$, and the carrier phase slips, $\Delta\varphi_{\text{ce}} = 2\pi f_{\text{CEO}} / f_{\text{rep}}$, are stable in the time domain. With stable values of T_R and $\Delta\varphi_{\text{ce}}$, we can perform a high-accuracy distant evaluation by calculating N and Δ from the separated MPTI fringes. If the MPTI fringes are sufficiently separated, Δ is measured as the distance between temporal coherence peaks of the MPTI fringes, and N is measured as the phase relation factor between the MPTI fringes. To avoid the overlapping of MPTI-fringes, another object mirror should be arranged at space position far away from the object mirror more than twice the FWHM (full width at half maximum) of the pulse. If MPTI-fringes are overlapped, the second object mirror should be used.

When only the pulse repetition frequency, f_{rep} , is steady, because the carrier phase slips, $\Delta\varphi_{\text{ce}}$, temporally changes, N cannot be decided from the MPTI fringes. In this case, we need to use a different method (for example, the ordinary TOF method) to evaluate N . With the knowledge of N , as indicated in Eq. (2), we can calculate Δ from the separated MPTI fringes to improve the measurement accuracy for performing a high-accuracy distant evaluation.

3. Experiment

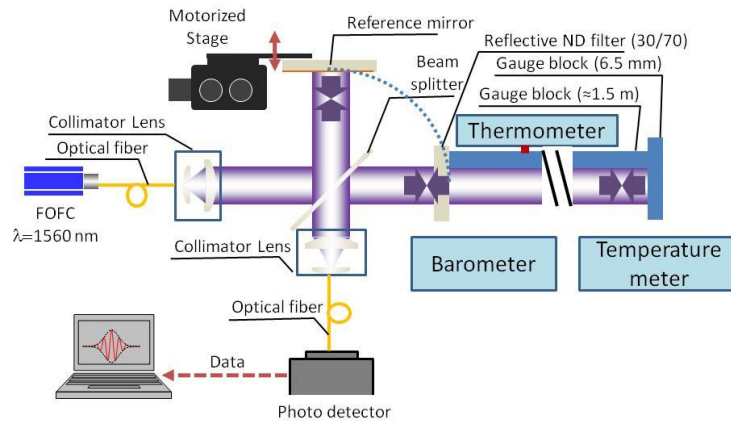


Fig. 3. Experimental setup used to demonstrate the feasibility of the MPTI-based TOF method.

As shown in Fig. 3, we used long gauge blocks as an already-known length in this experimental setup. The point was to compare the result of the proposed method with an already-known length to demonstrate the feasibility of the MPTI-based TOF method. If the reflected light on both sides of the long gauge block is recorded by MPTI fringes and the optical length difference is measured by MPTI fringes analysis, by comparing the result with the already-known value of the long gauge block, we can certificate the feasibility of the proposal method [18].

To provide the reflection on both sides of the long gauge block, one end of the long gauge block is wrung to a reflective ND filter and the far end of the long gauge block is wrung to a 6.5-mm gauge block. To make the intensity of the reflected light from the back surface of the reflective ND filter and the front surface of the 6.5-mm gauge block be almost the same, we used a 1.5-m long gauge block. The 1.5-m long gauge block is achieved by wringing three 500-mm gauge blocks (Mitsutoyo). The variations of tolerance of the central size of the three gauge blocks were $-0.42 \mu\text{m}$, $-0.50 \mu\text{m}$ and $-0.51 \mu\text{m}$, respectively. The thermal expansion coefficient of the gauge blocks was $(10.8 \pm 0.5) \times 10^{-6}/\text{K}$.

The optical experiment was carried out with an FOFC (FC1500, MenloSystems). To stabilize the repetition frequency, we introduced a repetition frequency stability unit RRE100

(MenloSystems). As a result, the repetition frequency achieved the stability of 10^{-9} order. We observed the repetition frequency with a frequency counter (IWATSU, SC-7206) as 100,000,000.0 Hz. The stability of the FOFC light source used in the experiment is 10^{-10} , which means spectral line width is about 100 kHz, and the temporal coherence length of the FOFC becomes 30 km.

The pulse trains from the FOFC were expanded and collimated by a collimator lens and introduced into the modified Michelson interferometer. As described above, two pairs of pulse trains traveled different path lengths and overlapped at the beam splitter. Another collimator lens made an image of the MPTI fringes on a photo detector via an optical fibre.

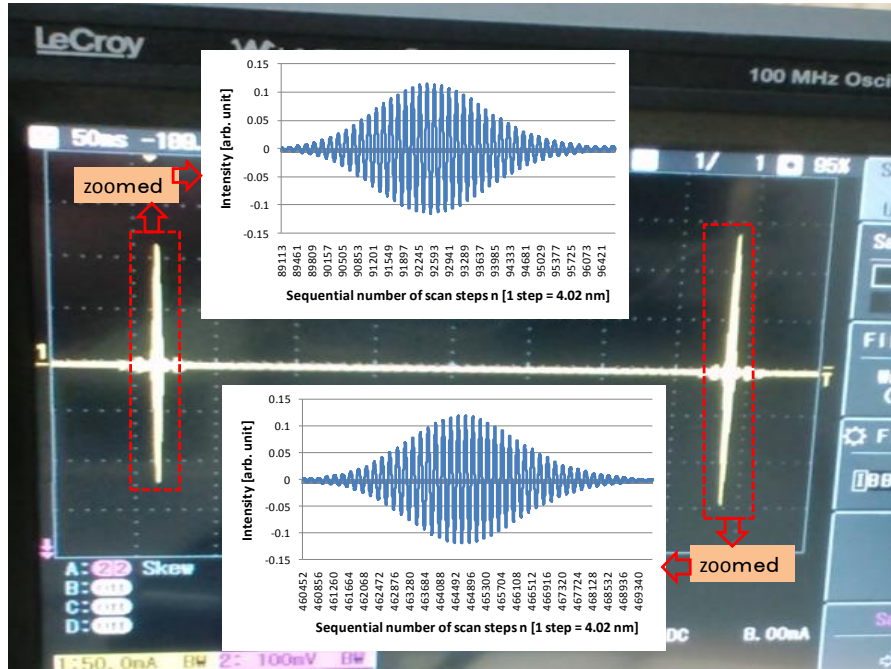


Fig. 4. A typical image of measured interference fringes.

Figure 4 illustrates the acquired interference fringes. Two interference fringe signals exhibited a high contrast between the two pairs of pulse trains by the relative optical displacements 0 and Δ , respectively. We confirmed the success of our interference system based on the proportion of the intensity of the MPTI fringes.

4. Results and discussion

The lengths of the long gauge block are listed in Table 1 with consideration of the temperature correction at eight times. The average length of the long gauge blocks was 1.500056289 m.

To obtain the length information of the long gauge block measured in air, as indicated in Eq. (1), we calculated $N \times c_n \times T_R / 2$ part and $\Delta / 2$ part. In this experiment, because the measurement object was relatively short, $N = 1$ was obtained by using a tape measure. The light velocity, $c_n = c / n$, was corrected according to the acquired temperature and the average humidity from the light velocity in the vacuum c . To calculate the refractive index of air, n , the humidity of air was assumed to be 50% and the acquired atmospheric pressure and the acquired temperature of air (23 °C) were used.

With the knowledge of the refractive index of air, n , the number of N and the repetition frequency $f_{\text{rep}} = 1/T_R$, we calculated $N \times c_n \times T_R / 2$, as shown in Table 2.

Table 1. Calibration for Long Gauge Blocks

No.	Temperature of the Gauge Block °C	Temperature Correction [m]	Length of the Gauge Block [m]
1	23.5765	0	1.500056655
2	23.575	-1.62×10^{-8}	1.500056639
3	23.5405	-3.888×10^{-7}	1.500056266
4	23.549	-2.97×10^{-7}	1.500056358
5	23.539	-4.05×10^{-7}	1.500056250
6	23.5205	-6.048×10^{-7}	1.500056050
7	23.509	-7.29×10^{-7}	1.500055926
8	23.531	-4.914×10^{-7}	1.500056164
Average			1.500056289

We calculated $\Delta/2$ part based on the distance between two temporal coherence function peaks using the Fourier transform technique [12]. Finally, by adding up $N \times c_n \times T_r / 2$ and $\Delta/2$, we acquired the length information of the long gauge block measured in air. Eight data sets were measured for each time block, and the average was assumed to be the measured length of the long gauge block.

Table 2. Calibration for the Length Information of the Long Gauge Block Measured in Air

No.	Atmospheric pressure [hPa]	Refractive index of air	$N \times c_n \times T_r / 2$ [m]	Length measurement in air [m]
1	1001.1	1.000262147	1.498569445	1.500065184
2	1001.8	1.000262331	1.498569169	1.500062906
3	1002.05	1.000262396	1.498569071	1.500065131
4	1002.3	1.000262462	1.498568973	1.500061685
5	1002.45	1.000262501	1.498568914	1.500061669
6	1002.85	1.000262606	1.498568757	1.500061363
7	1003.2	1.000262698	1.498568619	1.500061579
8	1003.2	1.000262698	1.498568619	1.500061148
Average				1.500062583

The average length of the long gauge block measured in air was 1.500062583 m, and the difference in the length of the long gauge block with consideration of the temperature correction was 6294 nm.

Figure 5 shows a comparison of measurement results.

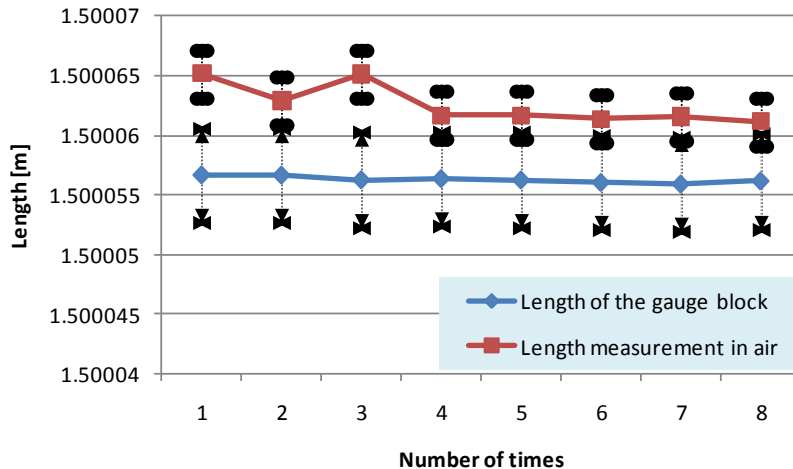


Fig. 5. Comparison of measurement results.

Both measured results of the length of the long gauge block correspond with consideration of the enhanced uncertainty of the optical measurement system. The reliability of the proposed method was confirmed by this long gauge block experiment.

The measurement resolution is about 4 nm, and is limited relatively by the resolution of the used oscilloscope (WaveJet 312A, LeCory).

The measurement uncertainty achievable in air using the MPTI fringes is 10^{-8} , because the uncertainty of Edlén Equation is 10^{-8} . The measurement uncertainty achievable in space using the MPTI fringes is $\Delta f_{\text{rep}}/f_{\text{rep}}$, because $\Delta T_n/T_n = \Delta f_{\text{rep}}/f_{\text{rep}}$. We will study on the measurement uncertainty in detail, and the results will be reported in the next paper.

The fringe acquisition time is about 30 seconds, and the post-processing time is about 30 seconds for one MPTI-fringes. The data update rate is about 1/60 Hz.

The experimental result suffers primarily from the measurement error of the temperature of the long gauge block, the temperature of air, and the atmospheric pressure due to the restrictions of the equipment available to us. The range of the measurement and the measurement time are fundamentally limited by the ability to scan the reference mirror. However, we want to stress that these limitations are not related to the principle itself. We are currently pursuing an approach in which performance can be improved using an optical device with high accuracy.

5. Conclusions

In conclusion, we proposed an MPTI-based TOF method whose unique feature is that high temporal coherence peaks between different pairs of pulse trains from the FOFC light source are used to record the two time points for the TOF method. When the offset shift frequency and the repetition frequency are stable, we can perform a high-accuracy arbitrary and absolute distant evaluation by calculating the phase relation factor between the MPTI fringes and the distance between temporal coherence peaks from the separated MPTI fringes. When only the repetition frequency is stable, the distance between temporal coherence peaks from the separated MPTI fringes can also be used to improve the measurement accuracy.

The proof-of-the-principle experiments, measuring the length of a long gauge block with the proposed optical method and comparing the result to the length of the long gauge block with consideration of the temperature correction, were presented, and the results validated the proposed principle. This is, to the best of our knowledge, the first report on the principle and the experimental demonstration of an MPTI-based TOF method. The present technique is

expected to be useful for the measurement of high-precision distances to fulfill science purposes and meet industry requirements.

Acknowledgments

This research work was financially supported by the “Development of System and Technology for Advanced Measurement and Analysis” Program at the Japan Science and Technology Agency (to H. M.) and the Global Center of Excellence Program on “Global Center of Excellence for Mechanical Systems Innovation” granted to the University of Tokyo, from the Japanese Government, respectively. D. W. gratefully acknowledges the scholarship given by Takayama International Education Foundation, Heiwa Nakajima Foundation, and Ministry of Education, Culture, Sports, Science, and Technology of Japan (MEXT), respectively.